



A continuous microwave/nZVI treatment system for malachite green removal: system setup and parameter optimization

Yanpeng Mao*, Jin Xu, Chunyuan Ma

National Engineering Laboratory of Coal-fired Pollutants Emission Reduction, School of Energy and Power Engineering, Shandong University, Jinan 250100, China, Tel. +86 53188399372; Fax: +86 53188395877; emails: maoyanpeng@sdu.edu.cn (Y. Mao), xuejn900826@qq.com (J. Xu), Tel. +86 53188399369; Fax: +86 53188395877; email: chym@sdu.edu.cn (C. Ma)

Received 10 September 2015; Accepted 7 January 2016

ABSTRACT

A continuous microwave/nZVI treatment system was built for the removal of malachite green (MG). Using the system, MG was efficiently degraded in a short hydraulic retention time. Operational parameters, including flow rate of influent, aeration method, microwave power (MP), and pH of MG solution, were optimized. The results indicate that the removal efficiency of MG increased significantly following the decrease in influent flow rate (Q_i). At $Q_i = 4$ mL/min, the highest removal efficiency of MG reaches 98.5%, while the highest load of MG degradation per gram of nZVI was 74.3 mg/g at $Q_i = 16$ mL/min. Increasing the MP could slightly increase MG and TOC removal efficiency. And analysis of system shock resistance indicated the use of this system stabilized effluent quality. It was further concluded that MG removal efficiency could benefit from pre-acidification processes to reach the pH range from 5.0 to 7.0 and pre-aeration prior to using the system. The dominant gas product and the residual detected following degradation of MG in the nZVI system were CO_2 and iron oxides, respectively.

Keywords: Microwave; nZVI; Malachite green; Continuous treatment

1. Introduction

The removal of organic dyes from wastewater is of major concern, especially in areas that are vulnerable to environment. Traditional approaches [1], including carbon adsorption, filtration, chemical precipitation, electrochemical treatment, and membrane technology, and novel approaches, such as photocatalytic decolorization using quantum dots (QDs) as nanophotocatalysts [2–4], are used to achieve satisfactory organic dyes removal. However, the organic dyes normally used in the textile industry exhibit anti-oxidation and

anti-photodecomposition properties [5], which makes the decolorization of organic dyes much more difficult.

Microwave (MW) irradiation has gained interest in the last few years as an efficient technique for water and wastewater treatment. However, the use of MW alone cannot achieve sufficient degradation of organics in wastewater treatment. MW-assisted methods, including MW with cooperated oxidants, catalysts, the Fenton process, and photocatalysis [6] for pollutant degradation, can dramatically reduce treatment time by increasing the degradation rate, providing the advantages of significantly smaller treatment reactor

*Corresponding author.

as well as easier and often more reliable *in situ* operation.

To date, studies on MW-enhanced catalytic degradation of organics in the presence of absorbers, semiconductors, ferromagnetic metals, or transition metal oxides have been conducted primarily in relation to the development of catalysts and mechanisms for degradation of organics. Several studies have employed MW radiation in combination with CoFe_2O_4 [7], MgFe_2O_4 [8], NiFe_2O_4 [9], CuFe_2O_4 [10], carbon [11–13], carbon-supported copper [14] and platinum [15], zero-valent iron (ZVI) [16–20], and nickel oxides [21–23] for the degradation of various pollutants. We previously reported a rapid and efficient technique for dye removal using MW/nanoscale ZVI (nZVI) [24]. However, little research has been conducted into continuous treatment systems at a laboratory scale, which may reduce possibility for industrialization of these methods.

In this study, a continuous MW/nZVI treatment system, equipped with an industrial-grade MW system, was setup. Malachite green (MG) was used as target pollutant. Parameter optimizations, including influent flow rate, aeration method, microwave power (MP), and pH of the MG solution, were carried out to ensure continuous and efficient wastewater treatment using the MW/nZVI system.

2. Materials and methods

2.1. Materials

Analytical grade reagents were used in all cases, and were purchased from Shanghai Chemical Reagents Company. MG ($\text{C}_{23}\text{H}_{25}\text{ClN}_2$), an organic dye, was used as the target contaminant. The three-dimensional (3D) molecular structure of MG is shown in Fig. 1. A background solution containing 2.0 mmol/L NaHCO_3 and 0.1 mol/L NaCl was prepared one week prior to the commencement of each experiment, to ensure that equilibrium was reached between the background solution and the atmosphere. The simulated organic wastewater was prepared prior to use, by dissolving MG in the background solution. The nZVI particles were prepared based on a liquid-phase chemical reduction method, which was described in detail in our previous study [24].

2.2. Experimental system

A diagrammatic sketch of the experimental setup is shown in Fig. 2. The MW system (WLD3S-03), with a frequency rating of 2,450 MHz and output power range of 0–1,600 W, was designed by Sanle Co., Ltd

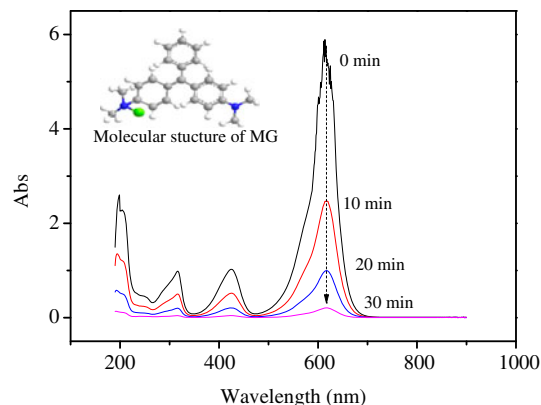


Fig. 1. The 3D molecular structure of MG and the qualitative analysis of MG UV-vis spectra at different time intervals after the continuous MW/nZVI treatment system at $C_0 = 100$ mg/L, MP = 600 W, pH 7.0, and $Q_g = 20$ mL (air)/min.

(Shanghai, China). MWs were generated by magnetrons and transferred via the waveguide into the MW cavity. To prevent damage to the magnetrons by the reflection of MWs, a circulator was placed between the MW generator and the MW cavity. It should be noted that the MW system used in this study was industrial grade, and could therefore run continuously without damaging the magnetrons.

The fixed bed quartz reactor (FBQR), shown in Fig. 3, was constructed from pure quartz (>99%), and could therefore tolerate temperatures of up to 1,000°C. The FBQR had a diameter of 20 mm and consisted of three parts: (1) a mixing section (50 mm tall) used for the mixing of liquid and gas; (2) a reaction section (80 mm tall), which was bounded by two quartz sand cores and filled with quartz fiber; and (3) a heat-exchange section (230 mm tall) used for preheating and cooling influent and effluent.

2.3. Experiment design

2.3.1. Continuous MW/nZVI treatment

Differing concentrations of MG solutions (100 and 200 mg/L), with varying pH values and 18 MΩ cm of ultrapure Milli-Q (MQ) water were stored in three Pyrex[®] vessels (1 L conical flask). The pH values of the MG solutions were adjusted using a PHS-3C pH meter (Shanghai, China) combined with a glass electrode and Ag/AgCl reference. Ten grams of nZVI particles were added into the FBQR, and MQ water and air were rapidly introduced for approximately 10 min to rinse the entire system. It should be noted that the comparative experiment of void column (without

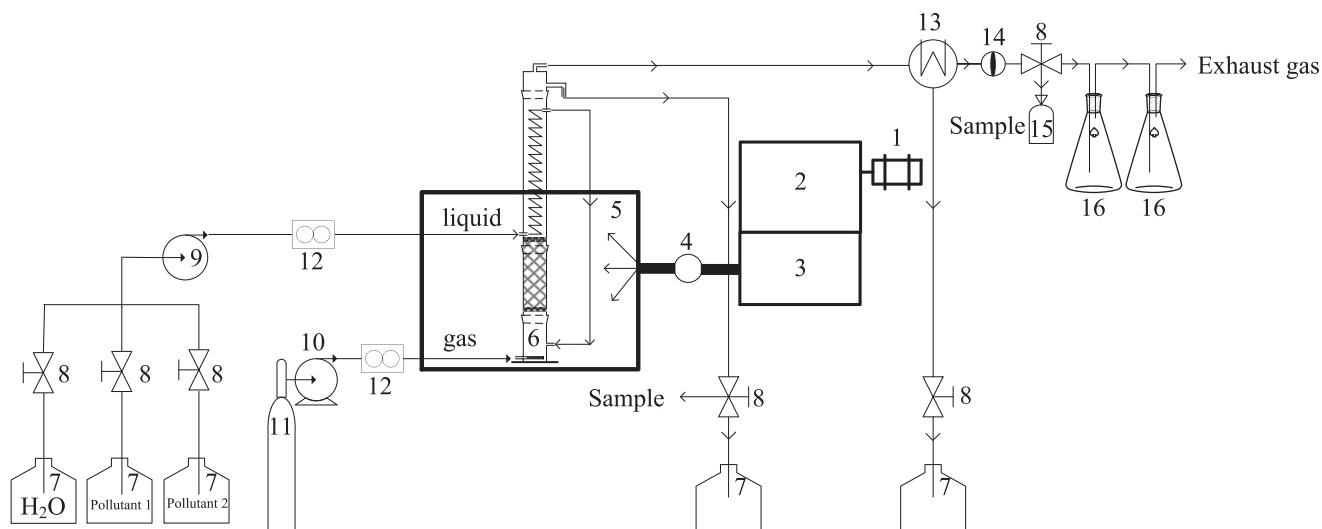


Fig. 2. Diagrammatic sketch of experimental setup equipped with MW system and gas and liquid paths, which include. Notes: (1) three-phase alternating-current source, (2) MW control instrument, (3) MW generator, (4) MW circulator, (5) MW cavity, (6) FBQR, (7) solution containers, (8) valves, (9) peristaltic pump, (10) air extracting pump, (11) gas cylinder, (12) flow meters, (13) heat exchanger, (14) dryer, (15) gas sampling bag, and (16) gas-absorbed bottles.

nZVI added) was not investigated in this study, as it has been found in our previous study [24] that only MW irradiation could not lead to any degradation of dye. After the rinsing process, the MG solution was pumped into the FBQR at different flow rates for 20 min. The MW system and stopwatch were then switched on simultaneously. The influent passed successively through sections 3, 1, 2, and 3, before being discharging into the solution container. The cleaned water, which was hot, could subsequently be reused in printing and dyeing processes if the system was commercialized. In the bottom section of the FBQR, gas was pumped at as low rate to achieve mixing and aeration. In the top section of the FBQR, the off-gas was purified successively by the heat exchanger and the dryer, and collected in the gas sampling bag. Finally, the exhaust gas was harmlessly discharged after absorption.

2.3.2. Parameter optimization

The parameters of the continuous MW/nZVI treatment system are shown in Table 1. The invariant parameters included the dimensions of FBQR and the dosage of nZVI. The ionic strength (I) and alkalinity (B) of the simulated organic wastewater were fixed at $I = 0.1$ mol/L NaCl and $B = 2.0$ mmol/L NaHCO_3 , respectively.

The hydraulic retention time (HRT) in section 2 is the most important parameter relating to the flow rate of influent (Q_i) in the system, and was varied from 1.0

to 6.4 min by changing the Q_i . To evaluate the effect of aeration gas on the removal of MG, different gases, including air, O_2 and N_2 were injected at the flow rate of gas (Q_g) of 20 mL/min. Additionally, different methods of aeration, including pre-aeration in the MG solution container and aeration in the FBQR, were investigated.

The effect of MP and pH of the MG solution on MG removal efficiency were investigated by increasing MP steadily from 0 to 1,000 W during the treatment, and varying the pH of MG solutions from 10.0 to 3.0. The shock resistance of the continuous MW/nZVI treatment system was investigated by abruptly changing the source of MG from the container with 100 mg/L MG to that with 200 mg/L MG.

MG and TOC removal efficiencies (R_M , % and R_T , %) were determined (as a percentage) at 10 min intervals, using Eq. (1):

$$R = \frac{C_0 - C_r}{C_0} \times 100 \quad (1)$$

where C_0 (mg/L) is the initial MG or TOC concentration and C_r (mg/L) is the residual MG or TOC concentration.

2.3.3. Chemical analysis of nZVI, off-gas and effluent

The morphology of the nZVI particles was observed with an EVO MA 15 (Zeiss, Germany) scanning electron microscope at 5 kV to characterize the

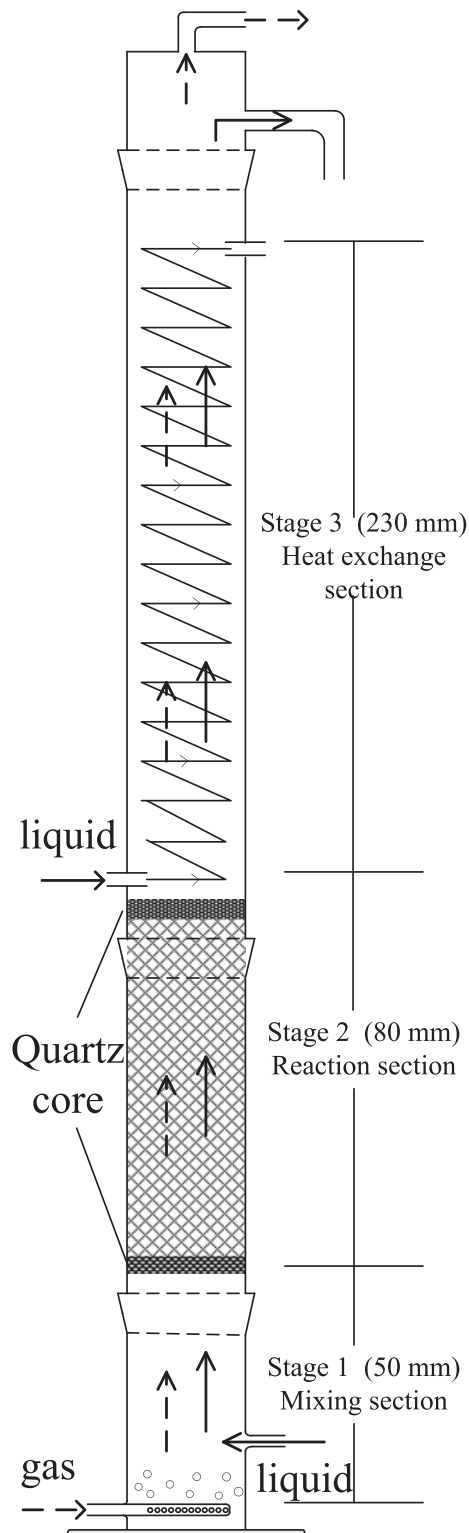


Fig. 3. Structure scheme of FBQR.

surface-changes in the metal particles. The chemical structure and functional groups in invalid nZVI

particles were determined using a Nicolet 6,700 Fourier transform infrared spectroscopy (FTIR, Thermo Fisher Scientific, USA). The wave number region ranged from 4,000 to 400 cm^{-1} , and the optical grade potassium bromide (KBr), dried at 80 °C for 8 h before use, was selected as a spectroscopic matrix. The main components of off-gas were detected via gas chromatographic spectrometry (PE580, PerkinElmer, USA).

The concentrations of MG in the different samples were measured using a UV–vis spectrophotometer (TU-1901, Persee, China) based on Beer-Lambert's law. The absorption spectrum of MG solutions, using full-wavelength scanning, qualitatively shows that the absorption maxima in the UV–vis spectra of MG solutions occur at 617 nm (Fig. 1). Therefore, calibration curves at each pH for determining the dye concentrations were developed based on the absorbance signal at 617 nm, giving rise to high r^2 values (>0.99). It should be noted that MG solution with high concentration should be diluted by several times until the absorbance at 617 nm was in the range of the calibration curve, and the value obtained from the calibration curve was multiplied by the dilution times, which gives the original concentration of MG solutions.

Total organic carbon (TOC) concentrations in effluent samples were tested using a TOC analyzer (Aurora 1030D, O.I., USA). The concentration of total soluble Fe (Fe_T) in dye samples was quantified with an inductively coupled plasma-emission spectrometer (OPTIMA 7000DV, PerkinElmer, USA).

3. Results

3.1. Effect of flow rate of influent on MG removal

The extent of MG removal, investigated as a function of time at differing flow rates of the influent ($Q_i = 4\text{--}24$ mL/min), was examined at $C_0 = 100$ mg/L, $MP = 600$ W, pH 7.0 and $Q_g = 20$ mL (air)/min. As shown in Fig. 4, the removal process of MG in the influent included three major stages, namely, the growth stage (<30 min), the stationary (30–140 min) stage and the decay stage (140–170 min). Clearly, the duration of the growth stage was correlated with Q_i , and higher Q_i would result in more rapid response of the MG concentration in the effluent, as the movement of MG solution in the FBQR was sequencing. However, the duration of the decay stage was not correlated with Q_i , which suggests that Q_i had little effect on the neutralization of nZVI in the FBQR.

It is evident from Fig. 4 that MG removal efficiency during the stationary stage increased gradually with the decrease in the Q_i , which was due to the increase

Table 1

Parameters of continuous MW/nZVI treatment system

Parameters of fixed bed quartz reactor	Diameter	20 mm
	Volume of section II	25.1 mL
	Flow rate of influent (Q_i)	<24.0 mL/min
	Hydraulic retention time in section II	>1.0 min
	Flow rate of gas (Q_g)	20 mL/min
	Dosage of nZVI	10 g
	Microwave power	0–1,000 W
Parameters of wastewater	Temperature	22°C
	pH	7.0–9.0
	NaCl	0.1 mol/L
	NaHCO ₃	2.0 mmol/L
	Malachite green	100 mg/L, 200 mg/L

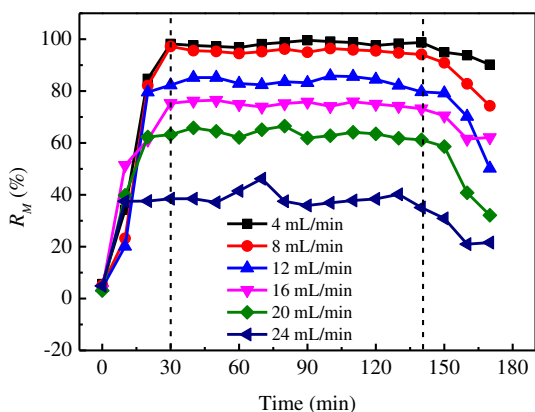


Fig. 4. The MG removal efficiency by continuous MW/nZVI treatment system as a function of time with different flow rates of influent at $C_0 = 100$ mg/L, MP = 600 W, pH 7.0, and $Q_g = 20$ mL (air)/min.

in the contact time between the MG molecules and nZVI in the FBQR when HRT was increased by maintaining a slower Q_i . The average MG removal efficiencies during the stationary stage from 30 to 140 min were 98.2, 95.5, 83.6, 75.0, 63.5, and 37.5% for Q_i equaling 4, 8, 12, 16, 20, and 24 mL/min, respectively. However, the growth rate of R_M decreased gradually when Q_i was increased. The following empirical equation was used to calculate the MG removal capacity of nZVI at $C_0 = 100$ mg/L, MP = 600 W, pH 7.0, and $Q_g = 20$ mL (air)/min:

$$L = \frac{(C_0 - \bar{C}_r) \times Q_i}{m} \quad (2)$$

where L (mg/g) is the MG degradation load per gram of nZVI, \bar{C}_r (mg/L) is the average residual MG concentration and m (g) denotes the mass of nZVI,

which is 10 g in this study. As shown in Fig. 5, L reaches the maximum value of 74.3 mg/g at $Q_i = 16$ mL/min, where average MG removal efficiency is only 75.0%.

Therefore, when a continuous MW/nZVI treatment system is used for advanced wastewater treatment, where high MG removal efficiency is necessary to meet strict discharge standards, slower Q_i should be used until the effluent satisfies the discharge standards. When the system is used for wastewater pretreatment, the Q_i of 16 mL/min could be applied to achieve the highest usage efficiency of nZVI.

3.2. Effect of aeration on MG removal

To evaluate the effect of aeration on MG removal, air, O₂ and N₂ aeration in the FBQR were investigated

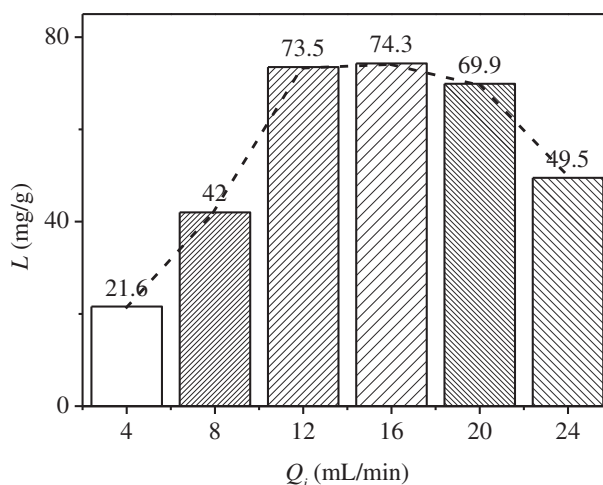


Fig. 5. The MG degradation load of per gram nZVI in the continuous MW/nZVI treatment system as a function of different flow rates of influent at $C_0 = 100$ mg/L, MP = 600 W, pH 7.0, and $Q_g = 20$ mL (air)/min.

(see Fig. 6). The efficiency of MG degradation increased nonlinearly with an increase in the oxygen content of aeration gas. Even N_2 aeration showed an MG removal efficiency of about 80.0%. This can be explained by the fact that N_2 aeration could not reject all the dissolved oxygen in the MG solution during short contact time between the aeration gas and the solution. However, the concentration of dissolved oxygen in real wastewater is very low as a consequence of aerobic degradation; hence aeration is necessary to improve the oxygen transfer efficiency in wastewater. In this study, pre-aeration using air in the MG solution was also investigated. As shown in Fig. 6, MG removal efficiency following air pre-aeration was similar to that of the air and O_2 aeration in the FBQR. Therefore, the effect of pre-aeration prior to continuous MW/nZVI treatment is considerable in practical applications where it is difficult to set up aeration in the FBQR.

Further, the results shown in Fig. 6 indicate that the duration of the decay stage increased when O_2 aeration was applied. This implies that the increase in oxygen content accelerated the neutralization of nZVI in the FBQR. Therefore, it is important to choose an aeration mode that optimizes both removal efficiency and operation costs. It also can be concluded that the oxidizing reactions of nZVI by O_2 occurred simultaneously during the degradation of MG around the nZVI hotspots in the FBQR. It has been demonstrated that the four-electron transfer between nZVI and O_2 induced the production of reactive oxygen species (ROS), which are capable of degrading organics in wastewater [25]. Hence, the degradation of MG in the FBQR would be brought about by not only thermal

decomposition around the nZVI hotspot, but also by non-thermal chemical reactions between ROS and MG. However, the presence of ROS was not detected in this study, and will be researched further in greater detail.

3.3. Effect of pH and MP on MG and TOC removal

The MG and TOC removal efficiencies by this system at a pH range from 3.0 to 10.0 have been investigated under the experimental conditions of $C_0 = 100$ mg/L, $MP = 600$ W, $Q_i = 4$ mL/min and $Q_g = 20$ mL (air)/min. As shown in Fig. 7, at lower pH from 3.0 to 5.0, the MG and TOC removal efficiencies were slightly increased following the increase of pH, which may be due to the fast consumption of nZVI at lower pH and high temperature. However, at higher pH from 7.0 to 10.0, decreasing the pH resulted in a slight increase in MG and TOC removal efficiencies, which is similar to that of our previous study on the removal of dyes by the MW/nZVI batch reactor [24], and to the trend observed for methyl orange removal [26] and nitrate removal using nZVI [27]. As most dye wastewater is strongly alkaline (higher than pH of 10), a process of pre-acidification prior to continuous MW/nZVI treatment to reach the pH range from 5.0 to 7.0 is suggested in this study, to increase the MG and TOC removal efficiencies. Evidence from the various cases indicated that TOC removal efficiency was lower than MG degradation efficiency (by approximately 10.1–22.0%). The results further indicated that MG was degraded in the continuous

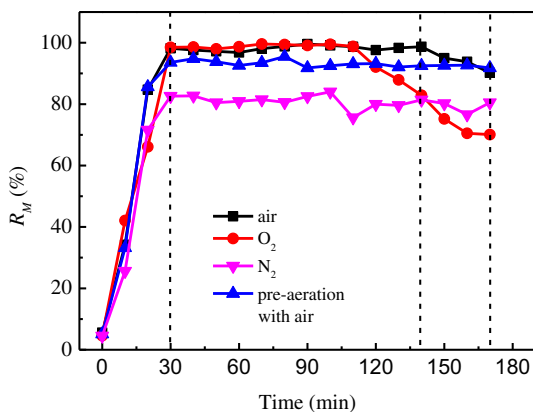


Fig. 6. The MG removal efficiency by continuous MW/nZVI treatment system as a function of time with different ways of aerations at $C_0 = 100$ mg/L, $MP = 600$ W, pH 7.0, $Q_i = 4$ mL/min, and $Q_g = 20$ mL (air)/min.

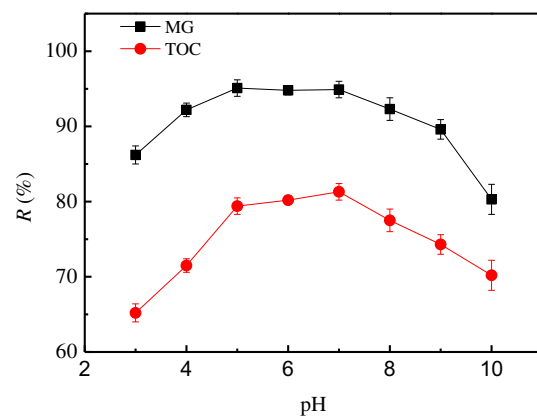


Fig. 7. The effect of pH on the MG and TOC removal efficiency by continuous MW/nZVI treatment system from pH range 3.0–10.0 at the experimental conditions of $C_0 = 100$ mg/L, $MP = 600$ W, $Q_i = 4$ mL/min, and $Q_g = 20$ mL (air)/min. Error bars are the standard error of the mean from the data obtained at different times (60–90 min) during continuous MW/nZVI treatment system.

MW/nZVI treatment system by producing a number of intermediates prior to mineralization, and that the use of MW radiation dramatically enhanced mineralization efficiency.

The effect of MP on MG and TOC removal efficiencies was investigated by varying the MP from 0 to 1,000 W at $C_0 = 100$ mg/L, pH 7.0, $Q_i = 8$ mL/min, and $Q_g = 20$ mL (air)/min. As shown in Fig. 8, the MG and TOC removal efficiencies were extremely low (less than 10%) during the initial 30 min when MW radiation was turned off, and the removal of MG and TOC occurred only through their adsorption onto nZVI. However, the use of MW radiation markedly increased MG and TOC removal efficiencies. It was also shown that removal efficiency increased nonlinearly with increase in MP. Furthermore, increasing MP from 400 to 1,000 W only enhanced the removal efficiency of MG from 85.6 to 91.9%, while that of TOC increased from 70.9 to 89.2%. The increase in TOC removal is greater than that for MG removal, indicating that more MG molecules in the solution were mineralized at a higher MP. As shown in Fig. 8, the experimental results also indicated that the TOC removal efficiency or the mineralization of MG dropped sharply during the decay stage, possibly due to the low mineralization efficiency caused by the neutralized nZVI.

3.4. Shock resistance of the continuous MW/nZVI treatment system

The shock resistance of the continuous MW/nZVI treatment system was investigated by abruptly changing the MG source from the container with 100 mg/L

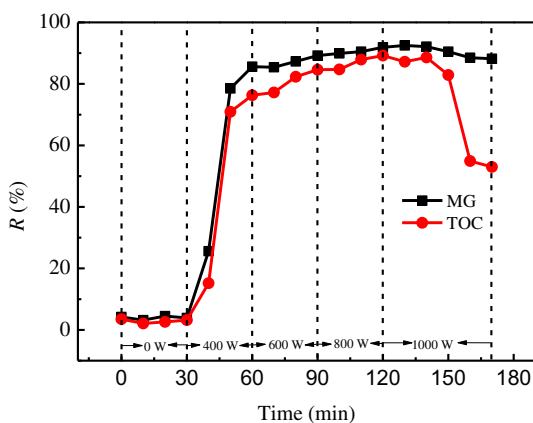


Fig. 8. The MG and TOC removal efficiency by continuous MW/nZVI treatment system as a function of time with varying MP from 0 to 1,000 W at $C_0 = 100$ mg/L, pH 7.0, $Q_i = 8$ mL/min, and $Q_g = 20$ mL (air)/min.

MG to that with 200 mg/L MG at MP = 600 W, pH 7.0, $Q_i = 8$ mL/min and $Q_g = 20$ mL (air)/min. Furthermore, the data in Fig. 9 demonstrate that the continuous MW/nZVI treatment system has high shock resistance and therefore the capability to maintain high MG removal efficiency and stabilize effluent concentrations.

4. Discussion

4.1. Speciation of off-gas

The species of off-gas produced in the continuous MW/nZVI treatment system were examined using gas chromatographic spectrometry with a thermal conductivity detector and He carrier gas. The spectra results when using O_2 and N_2 aeration are shown in Fig. 10. The characteristic CO_2 peak appeared in all scenarios, suggesting CO_2 production during MG degradation in the continuous MW/nZVI treatment system. It should be noted that when using N_2 aeration, both CO_2 and O_2 showed smaller peak values, probably resulting from the rejection of O_2 from the MG solutions as a consequence of N_2 aeration. In Fig. 10(a), the characteristic peaks during the initial 10 min appear more complicated than those at 60 and 120 min, possibly due to the incomplete degradation of MG into smaller molecules. The above results evidenced that the mineralization of MG is essential in MG degradation using the continuous MW/nZVI treatment system, and that the dominant species produced in off-gas is CO_2 , which can be discharged harmlessly into the atmosphere.

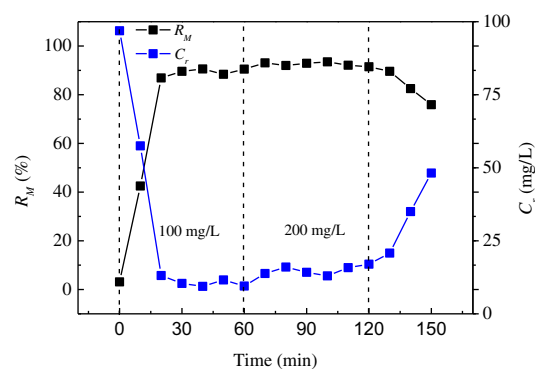


Fig. 9. The shock resistance of the continuous MW/nZVI treatment system at MP = 600 W, pH 7.0, $Q_i = 8$ mL/min, and $Q_g = 20$ mL (air)/min. The MG source from the container with 100 mg/L MG was changed to that with 200 mg/L MG at $t = 60$ min.

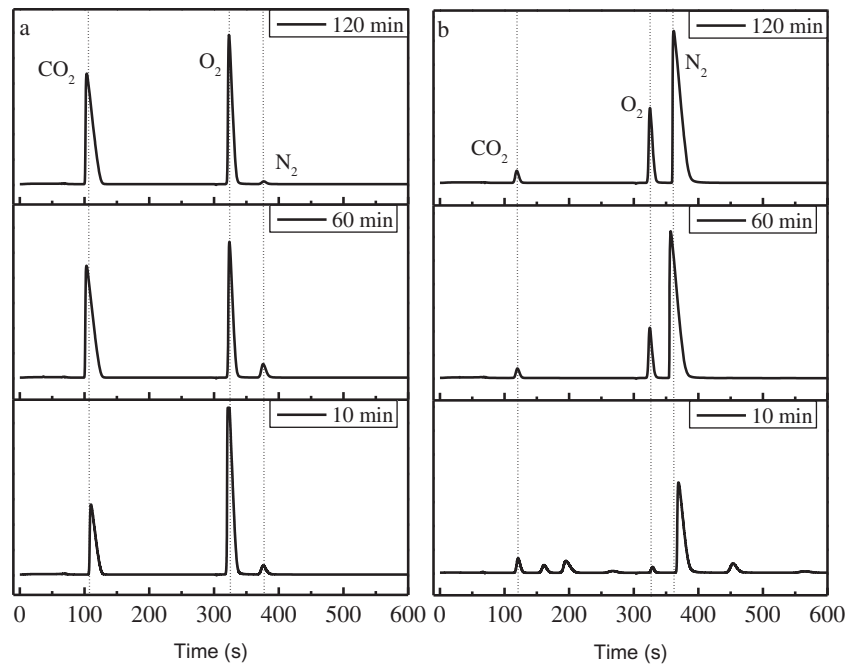


Fig. 10. The gas chromatographic spectra of the off-gases from O₂ (a) and N₂ (b) aeration.

4.2. Speciation of iron in the system

In our previous study [24], soluble iron species could be formed in the MW/nZVI treatment system via the two-electron transfer between nZVI and oxygen. In this study, the total iron in the effluent was measured and the distribution of iron in solid and liquid phases was calculated. Fig. 11 describes the effect of Q_i on the concentration of Fe_T in the effluent and the distribution of iron in solid and liquid phases. As can be seen, slight decrease in the concentration of Fe_T occur when the amount of effluent is increased. Additionally, a small portion of iron was found in the liquid phase (less than 0.51 g) in different experimental situations, although speciation using the Visual Minteq 3.0 chemical equilibrium program [28] indicated that all Fe(III) would be precipitated at the pH level examined in this study.

Most of the iron stayed in the solid phase, and hence the SEM and FTIR of the nZVI and the solids following MG treatment (nZVI_a) were investigated (see Figs. 12 and 13). The SEM image of the nZVI showed perfectly spherical particles of diameter < 200 nm. However, the SEM image of the nZVI_a was observed as an agglomerate, and the spherical nZVI particles disappeared. The FTIR spectra of both nZVI and nZVI_a exhibited adsorption bands around 3,400 cm⁻¹, indicating O–H stretching of the hydroxyl group and hydrogen bonds, which were related to a

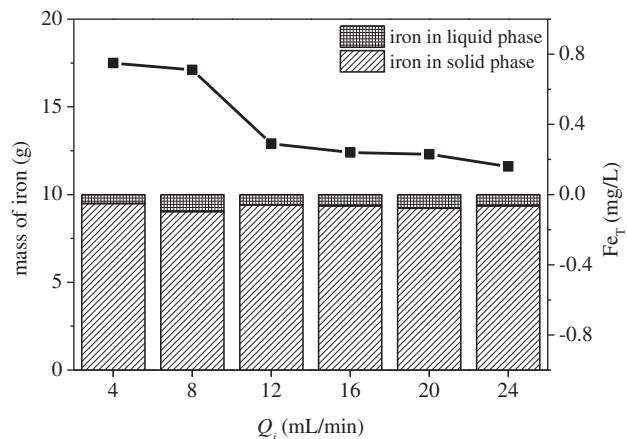


Fig. 11. Effect of influent flow rate on the distribution of iron in solid or liquid phase (bars) and the concentration of total iron in effluent (solid line) at $C_0 = 100$ mg/L, MP = 600 W, pH 7.0, and $Q_g = 20$ mL (air)/min.

peak at the range of 3,200–3,600 cm⁻¹ [29,30]. The absorption peaks around 1,560 and 1,400 cm⁻¹ of nZVI might indicate the presence of C–O and B–O, likely related to the preparation of nZVI using NaBH₄ and starch. The absorption peaks at 1,186, 1,049, and 470 cm⁻¹ were similar to the characteristic peaks of iron oxides [31–33], indicating oxidation of nZVI during MG treatment.

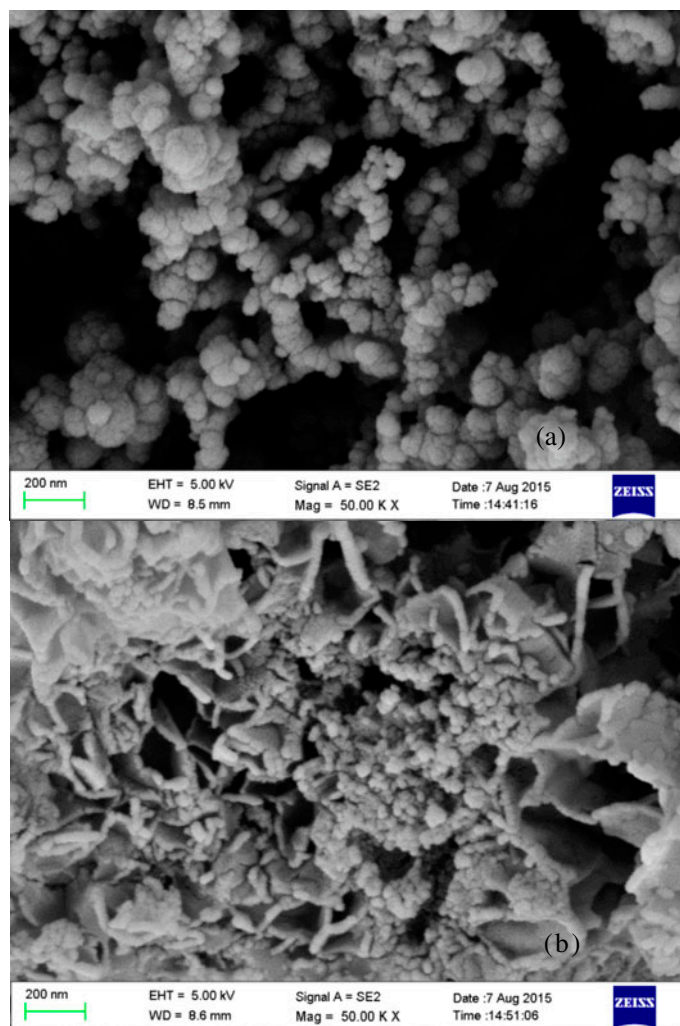


Fig. 12. The SEM of nZVI (a) and the solid after MW/nZVI treatment (b).

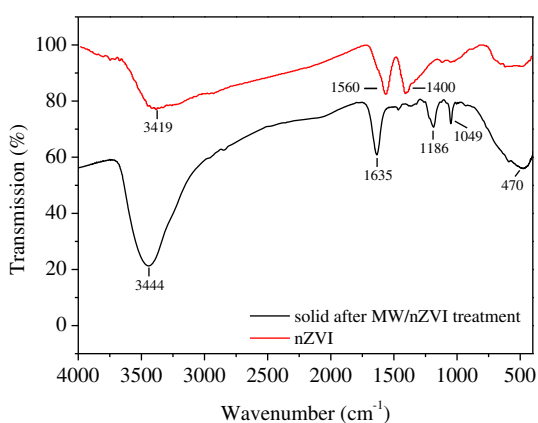


Fig. 13. The FTIR spectra of nZVI and the solid after MW/nZVI treatment.

5. Conclusion

A continuous MW/nZVI treatment system was built for this study. The MG removal capacity of the system was investigated, and parameters were optimized. The results demonstrate that the continuous system could efficiently degrade and mineralize the target pollutant with a very short HRT, possibly leading to a very convenient *in situ* treatment for pollutants at contaminated sites. The results also indicate that pre-acidification process prior to using the continuous system to reach the pH range from 5.0 to 7.0, and both of air pre-aeration and air or O₂ aeration in the FBQR could enhance the degradation efficiency of pollutants. Furthermore, the system exhibits high shock-resistance. The dominant gas products of the system were CO₂ and H₂O, which can be discharged directly into atmosphere without any risk to health.

Most of the nZVI was oxidized and stayed in the solid phase after treatment, and the concentration of iron in the effluent was extremely low.

The continuous system could be conveniently used, within a small area, for pretreatment of highly concentrated organic wastewater, and as an advance treatment for water reuse. However, notwithstanding its high potential, factors such as energy and nZVI consumption would increase the cost of wastewater treatment. Therefore, the application of the system could benefit from improved MW energy efficiency and substitutes for nZVI. The continuous system with parameters developed in our study was investigated in the simulated dye wastewaters containing simple inorganic matrices. In real wastewater, various electrolytes, such as sulfate, nitrate, and phosphate, may affect the dye removal efficiency in some extent. In addition, organic dyes could complex metal ions, and the formed dye–metal species would also affect the dye reduction. Hence, in these cases, a detailed understanding of the reactions between the dyes and nZVI under MW radiation, which would be useful to explain the effect of different electrolytes, should also be investigated in the future.

Acknowledgments

We gratefully acknowledge financial support from the Postdoctoral Science Foundation of China (2013M531602), and the National Natural Science Foundation of China (21307075).

References

- [1] A. Latif, S. Noor, Q.M. Sharif, M. Najeebullah, Different techniques recently used for the treatment of textile dyeing effluents: A review, *J. Chem. Soc. Pakistan* 32 (2010) 115–124.
- [2] H.R. Rajabi, M. Farsi, Quantum dot based photocatalytic decolorization as an efficient and green strategy for the removal of anionic dye, *Mater. Sci. Semicond. Process.* 31 (2015) 478–486.
- [3] H.R. Rajabi, M. Farsi, Effect of transition metal ion doping on the photocatalytic activity of ZnS quantum dots: Synthesis, characterization, and application for dye decolorization, *J. Mol. Catal. A: Chem.* 399 (2015) 53–61.
- [4] H.R. Rajabi, O. Khani, M. Shamsipur, V. Vatanpour, High-performance pure and Fe³⁺-ion doped ZnS quantum dots as green nanophotocatalysts for the removal of malachite green under UV-light irradiation, *J. Hazard. Mater.* 250–251 (2013) 370–378.
- [5] M. Tichonovas, E. Krugly, V. Racys, R. Hippler, V. Kauneliene, I. Stasiulaitiene, D. Martuzevicius, Degradation of various textile dyes as wastewater pollutants under dielectric barrier discharge plasma treatment, *Chem. Eng. J.* 229 (2013) 9–19.
- [6] N. Remya, J.-G. Lin, Current status of microwave application in wastewater treatment—A review, *Chem. Eng. J.* 166 (2011) 797–813.
- [7] L. Zhang, M. Su, X. Guo, Studies on the treatment of brilliant green solution by combination microwave induced oxidation with CoFe₂O₄, *Sep. Purif. Technol.* 62 (2008) 458–463.
- [8] L. Zhang, X. Zhou, X. Guo, X. Song, X. Liu, Investigation on the degradation of acid fuchsin induced oxidation by MgFe₂O₄ under microwave irradiation, *J. Mol. Catal. A: Chem.* 335 (2011) 31–37.
- [9] L. Zhang, X. Liu, X. Guo, M. Su, T. Xu, X. Song, Investigation on the degradation of brilliant green induced oxidation by NiFe₂O₄ under microwave irradiation, *Chem. Eng. J.* 173 (2011) 737–742.
- [10] X. Liu, S. An, W. Shi, Q. Yang, L. Zhang, Microwave-induced catalytic oxidation of malachite green under magnetic Cu-ferrites: New insight into the degradation mechanism and pathway, *J. Mol. Catal. A: Chem.* 395 (2014) 243–250.
- [11] Y. Sun, Y. Zhang, X. Quan, Treatment of petroleum refinery wastewater by microwave-assisted catalytic wet air oxidation under low temperature and low pressure, *Sep. Purif. Technol.* 62 (2008) 565–570.
- [12] L. Bo, X. Quan, S. Chen, H. Zhao, Y. Zhao, Degradation of p-nitrophenol in aqueous solution by microwave assisted oxidation process through a granular activated carbon fixed bed, *Water Res.* 40 (2006) 3061–3068.
- [13] X. Liu, X. Quan, L. Bo, S. Chen, Y. Zhao, Simultaneous pentachlorophenol decomposition and granular activated carbon regeneration assisted by microwave irradiation, *Carbon* 42 (2004) 415–422.
- [14] L.L. Bo, Y.B. Zhang, X. Quan, B. Zhao, Microwave assisted catalytic oxidation of p-nitrophenol in aqueous solution using carbon-supported copper catalyst, *J. Hazard. Mater.* 153 (2008) 1201–1206.
- [15] L. Bo, X. Quan, X. Wang, S. Chen, Preparation and characteristics of carbon-supported platinum catalyst and its application in the removal of phenolic pollutants in aqueous solution by microwave-assisted catalytic oxidation, *J. Hazard. Mater.* 157 (2008) 179–186.
- [16] C.L. Lee, C.J.G. Jou, Degradation of chlorobenzene with microwave-aided zerovalent iron particles, *Environ. Eng. Sci.* 29 (2011) 432–435.
- [17] C.L. Lee, C.J. Jou, H.P. Wang, Enhanced degradation of chlorobenzene in aqueous solution using microwave-induced zero-valent iron and copper particles, *Water Environ. Res.* 82 (2010) 642–647.
- [18] C.J. Jou, Degradation of pentachlorophenol with zerovalence iron coupled with microwave energy, *J. Hazard. Mater.* 152 (2008) 699–702.
- [19] J. Fu, Z. Xu, Q.S. Li, S. Chen, S.Q. An, Q.F. Zeng, H.L. Zhu, Treatment of simulated wastewater containing Reactive Red 195 by zero-valent iron/activated carbon combined with microwave discharge electrodeless lamp/sodium hypochlorite, *J. Environ. Sci.* 22 (2010) 512–518.
- [20] N. Remya, J.G. Lin, Microwave-assisted carbofuran degradation in the presence of GAC, ZVI and H₂O₂: Influence of reaction temperature and pH, *Sep. Purif. Technol.* 76 (2011) 244–252.

- [21] T.L. Lai, J.Y. Liu, K.F. Yong, Y.Y. Shu, C.B. Wang, Microwave-enhanced catalytic degradation of 4-chlorophenol over nickel oxides under low temperature, *J. Hazard. Mater.* 157 (2008) 496–502.
- [22] T.L. Lai, W.F. Wang, Y.Y. Shu, Y.T. Liu, C.B. Wang, Evaluation of microwave-enhanced catalytic degradation of 4-chlorophenol over nickel oxides, *J. Mol. Catal. A: Chem.* 273 (2007) 303–309.
- [23] H. He, S. Yang, K. Yu, Y. Ju, C. Sun, L. Wang, Microwave induced catalytic degradation of crystal violet in nano-nickel dioxide suspensions, *J. Hazard. Mater.* 173 (2010) 393–400.
- [24] Y. Mao, Z. Xi, W. Wang, C. Ma, Q. Yue, Kinetics of Solvent Blue and Reactive Yellow removal using microwave radiation in combination with nanoscale zero-valent iron, *J. Environ. Sci.* 30 (2015) 164–172.
- [25] H.Y. Shu, M.C. Chang, H.H. Yu, W.H. Chen, Reduction of an azo dye Acid Black 24 solution using synthesized nanoscale zerovalent iron particles, *J. Colloid Interface Sci.* 314 (2007) 89–97.
- [26] J. Fan, Y. Guo, J. Wang, M. Fan, Rapid decolorization of azo dye methyl orange in aqueous solution by nanoscale zerovalent iron particles, *J. Hazard. Mater.* 166 (2009) 904–910.
- [27] G.C.C. Yang, H.L. Lee, Chemical reduction of nitrate by nanosized iron: Kinetics and pathways, *Water Res.* 39 (2005) 884–894.
- [28] J.P. Gustafsson, *Visual MINTEQ*, 2004.
- [29] A. Gupta, S.R. Vidyarthi, N. Sankararamakrishnan, Thiol functionalized sugarcane bagasse—A low cost adsorbent for mercury remediation from compact fluorescent bulbs and contaminated water streams, *J. Environ. Chem. Eng.* 2 (2014) 1378–1385.
- [30] M. Mahramanlioglu, I. Kizilcikli, I.O. Bicer, Adsorption of fluoride from aqueous solution by acid treated spent bleaching earth, *J. Fluorine Chem.* 115 (2002) 41–47.
- [31] P.W. Schindler, Co-adsorption of metal ions and organic ligands; formation of ternary surface complexes, *Rev. Miner. Geochem.* 23 (1990) 281–307.
- [32] M. Cagnasso, V. Boero, M.A. Franchini, J. Chorover, ATR-FTIR studies of phospholipid vesicle interactions with α -FeOOH and α -Fe₂O₃ surfaces, *Colloids Surf., B: Biointerfaces* 76 (2010) 456–467.
- [33] T. Nur, P. Loganathan, T.C. Nguyen, S. Vigneswaran, G. Singh, J. Kandasamy, Batch and column adsorption and desorption of fluoride using hydrous ferric oxide: Solution chemistry and modeling, *Chem. Eng. J.* 247 (2014) 93–102.